ISSN 1063-7834, Physics of the Solid State, 2019, Vol. 61, No. 10, pp. 1736–1745. © Pleiades Publishing, Ltd., 2019.
Russian Text © The Author(s), 2019, published in Fizika Tverdogo Tela, 2019, Vol. 61, No. 10, pp. 1783–1792.

MAGNETISM

Dynamics of Pulsed Remagnetization of Magnetically Uniaxial Nanoparticles

A. M. Shutyi[a], * and D. I. Sementsov[a]

[a] *Ulyanovsk State University, Ulyanovsk, 432000 Russia*

**e-mail: shuty@mail.ru*

Received April 7, 2019; revised May 5, 2019; accepted May 14, 2019

Abstract—The response of the magnetic moment of a magnetically uniaxial nanoparticle and a planar array of such nanoparticles to a short Gaussian magnetic field pulse is studied in the presence and absence of its modulation. The periodic dependence of the response duration and the final orientation of magnetic moments on the pulse duration and its peak value are revealed and analyzed. The effect of the weak bias magnetic field and the pulse field deviation from the transverse orientation on remagnetization processes is studied. It was shown that the effect of the dipole–dipole interaction leads to modulation of the response to the pulse exposure.

Keywords: pulsed remagnetization, precession dynamics, uniaxial anisotropy, magnetic nanoparticle

DOI: 10.1134/S1063783419100330

1. INTRODUCTION

In the last few decades, significant progress is being made in understanding properties and dynamic processes in magnetic nanoparticle systems [1–7]. Due to small sizes, magnetic nanoparticles are as a rule single-domain, which makes it possible to simplify the description of structures on their basis. The main contribution to the interaction of nanoparticles is made by the dipole–dipole interaction controlled not only by their intrinsic magnetic moment, but also local ordering of particles, as well as magnetic anisotropy [8–11]. The nanoparticle array structure discreteness leads to significant differences of equilibrium states and dynamic remagnetization from similar properties of macroscopic single-domain objects [12–14]. Among such differences can be, e.g., bistable array states caused by the existence of various equilibrium orientation configurations.

The possibility of data recording on magnetic dipole arrays is based on changing the equilibrium configuration of magnetic moments due to the effect of magnetic field pulses [15, 16]. Therefore, a significant number of both theoretical and experimental studies are devoted to pulsed remagnetization of magnetic micro- and nanosystems [17–26]. For example, the periodicity of the implementation of remagnetization of a planar layered microstructure with varying the pulse duration and amplitude was experimentally detected in [17], which was explained by the dominant role of phase coherence between the magnetization and field pulse during switching. In [18], the precession response of the microscopic memory cell magnetization to the pulse exposure is experimentally studied; therewith, cells with short switching times were detected, where long-wavelength magnetic excitations are suppressed after field pulse damping. In [19–22], the dynamics of antiferromagnetic system magnetization under exposure to ultrafast magnetic field pulses was studied. In particular, in [19], the possibility of system remagnetization with long relaxation process was shown; in [22], the possibility of remagnetization without long relaxation process using a special field signal shape was shown. Based on the Landau–Lifshitz equation, single-domain nanoparticle magnetization switching was considered in [23] and a scheme for setting the system to a given state using ultrashort magnetic pulses was proposed. In [24–26], pulsed remagnetization of films with various magnetic anisotropy types was studied, and dynamic hysteresis loops and relaxation effects during pulsed remagnetization of nanoparticles were considered.

In this study, based on the numerical solution of dynamic equations, the response to the Gaussian pulse of the magnetic field of the magnetic moment of an isolated nanoparticle with uniaxial anisotropy and a planar array of similar nanoparticles is studied. The conditions of pulsed remagnetization of dipoles and the effect of the response dynamics of the dipole–dipole interaction between array elements are determined. The consideration of a wide range of the pulse duration and peak value and the construction of corresponding diagrams allowed the detection of periodic dependences of both the magnetic moment precession response duration and the implementation of

nanoparticle remagnetization on pulse parameters. The effect of a weak static field, a pulse field deviation from the transverse orientation, and working pulse modulation on pulsed remagnetization of nanoparticles is studied.

2. BASIC EQUATIONS

Let us consider a planar array of 6 × 6 identical close-to-spherical nanoparticles with magnetic moment $|\mathbf{m}_i| = m$. Suppose that nanoparticles are arranged at sites of a square array with parameter r_0. Each nanoparticle features uniaxial magnetic anisotropy and has a size at which it is in the single-domain state. Let us write the i-th nanoparticle energy as the sum of the Zeeman energy in the external magnetic field $\mathbf{H}$, the dipole–dipole interaction energy, and the anisotropy energy

$$W(\mathbf{m}_i) = -\mathbf{m}_i\mathbf{H} + W_d(\mathbf{m}_i, \mathbf{m}_n) + W_a(\mathbf{m}_i). \quad (1)$$

Here the external magnetic field is the sum of static and high-frequency fields. The dipole–dipole interaction energy is given by

$$W_d(\mathbf{m}_i, \mathbf{m}_n) = \sum_{n\neq i}\left(\frac{\mathbf{m}_i\mathbf{m}_n r_{in}^2 - 3(\mathbf{m}_i\mathbf{r}_{in})(\mathbf{m}_n\mathbf{r}_{in})}{r_{in}^5}\right), \quad (2)$$

where $\mathbf{r}_{in}$ and r_{in} are the radius vector and the distance between ith and nth dipoles. The uniaxial anisotropy energy is given by

$$W_a(\mathbf{m}_i) = -K_u V_0 \frac{(\mathbf{m}_i\mathbf{n})^2}{m_i^2}, \quad (3)$$

where K_u and $\mathbf{n}$ are the uniaxial anisotropy constant and the unit vector of the easy magnetization axis (EMA), V_0 is the nanoparticle volume.

The dynamics of each dipole array moment is described by the Landau–Lifshitz equation with the relaxation term in the Hilbert form [27],

$$\frac{\partial\mathbf{m}_i}{\partial t} = -\gamma\mathbf{m}_i \times \mathbf{H}_i^{\text{eff}} - \frac{\alpha}{m_i}\mathbf{m}_i \times \frac{\partial\mathbf{m}_i}{\partial t}, \quad (4)$$

where γ is the gyromagnetic ratio and α is the dissipation parameter. The effective magnetic field induced in the i-th dipole position by other dipoles and external field $\mathbf{H}$, taking into account Eq. (1), is written as

$$\mathbf{H}_i^{\text{eff}} = -\frac{\partial W_i}{\partial\mathbf{m}_i} = \mathbf{H} + K_u V_0 \frac{\mathbf{n}(\mathbf{m}_i\mathbf{n})}{m_i^2} + \sum_{n\neq i}\frac{3(\mathbf{m}_n\mathbf{r}_{in})\mathbf{r}_{in} - \mathbf{m}_n r_{in}^2}{r_{in}^5}. \quad (5)$$

Then we pass to the dimensionless parameters $\boldsymbol{\mu}_i = \mathbf{m}_i/m$, $\mathbf{e}_{in} = \mathbf{r}_{in}/r_{in}$, $\tau = \gamma J t$, $l_{in}^3 = r_{in}^3/V_0$, where $J = m/V_0$ is the nanoparticle magnetization.

The dimensionless array parameter, i.e., the distance between centers of the nearest nanoparticles, $\rho = r_0 V_0^{-1/3}$. In dimensionless parameters, Eqs. (4) take the form

$$\frac{\partial\boldsymbol{\mu}_i}{\partial\tau} = -\boldsymbol{\mu}_i \times \mathbf{h}_i^{\text{eff}} - \alpha_i\boldsymbol{\mu}_i \times \frac{\partial\boldsymbol{\mu}_i}{\partial\tau}, \quad (6)$$

where

$$\mathbf{h}_i^{\text{eff}} = \mathbf{h} + k_u\mathbf{n}(\boldsymbol{\mu}_i\mathbf{n}) + \sum_{n\neq i}\left[\frac{3(\boldsymbol{\mu}_n\mathbf{e}_{in})\mathbf{e}_{in} - \boldsymbol{\mu}_n}{l_{in}^3}\right].$$

In this case, the undimensioned external field and uniaxial anisotropy constant take the form $\mathbf{h} = \mathbf{H}/J$, $k_u = K_u/J^2$.

Let us write the transition from dimensionless to dimensional quantities for the dipole nanoparticle array consisting of N iron atoms: the nanoparticle magnetic moment $m \approx 2.2\mu_B$, where μ_B is the Bohr magneton. For example, for a stable spherical configuration, $N = 561$ and the nanoparticle radius is $R = 1.364 \times 10^{-7}$ cm, $m \approx 1.145 \times 10^{-17}$ erg/Oe, and $J \approx 1.08$ kG. Taking into account $\gamma = 1.76 \times 10^7$ (Oe s)$^{-1}$, we find the following numerical evaluations for the time $t = \tau/(\gamma J) \approx 0.53\tau$ ps, magnetic field $H = Jh \approx 1.08h$ kOe, and anisotropy constant $K_u = J^2 k_u \approx 1.2 \times 10^6 k_u$ erg/cm^3.

In the subsequent analysis, vector equation (6) is represented by three scalar equations. For example, for x-components of $\partial\boldsymbol{\mu}_i/\partial\tau$, we obtain

$$(1+\alpha^2)\frac{\partial\mu_{ix}}{\partial\tau} = (\mu_{iz} + \alpha\mu_{ix}\mu_{iy})h_{iy}^{\text{eff}} - (\mu_{iy} - \alpha\mu_{iz}\mu_{ix})h_{iz}^{\text{eff}} - \alpha(1-\mu_{ix}^2)h_{ix}^{\text{eff}}. \quad (7)$$

Equations for other components similar forms and can be obtained by cyclic permutation of components.

Below let us consider both an isolated nanoparticle and a 6 × 6 array of identical nanoparticles. The coordinate system was selected so that the X axis is perpendicular to the array planes, and two other axes are parallel to array sides. The EMA direction coincides with the Y axis, the anisotropy constant is taken as $k_u = 1$. The dissipation parameter is set to $\alpha = -0.01$.

Equilibrium orientations and precession dynamic modes of the total magnetic moment of the array are determined based on a numerical analysis performed using the Runge–Kutta method.

3. MAGNETIC MOMENT RESPONSE TO THE MAGNETIC FIELD PULSE

Let us consider the response of an isolated nanoparticle to the Gaussian magnetic field pulse

$$h(\tau) = h_0 \exp[-(\tau - \tau_i)^2/2\tau_0^2], \quad (8)$$

where h_0, τ_i, and τ_0 are the peak field, temporal shift of the pulse maximum and the pulse duration; in what follows, we set $\tau_i = 200$. In the case without bias mag-

netic field or under a relatively weak field ($h_y \ll k_u$) directed along the EMA, the conditions of the implementation of nanoparticle remagnetization are periodically satisfied with varying the pulse duration (or peak value).

For a bias magnetic field polarized along the Y axis, Figs. 1a–1c (h_y = 0.1, 0, –0.1) show the diagrams reflecting the dependence of the remagnetization implementation on the Gaussian pulse amplitude and duration, in which dark areas correspond to remagnetization implementation at given pulse parameters, bright areas correspond to the absence of remagnetization. In the initial state, the nanoparticle magnetic moment is oriented in the positive Y axis direction. The diagrams show that the remagnetization implementation periodicity takes place with varying the pulse duration and amplitude, and the period of corresponding intervals decreases with increasing parameters. In the case without bias magnetic field (b) at sufficiently high pulse parameters, an approximate equality between interval corresponding to remagnetization and its absence takes place. In the case of a weak bias magnetic field codirected to the magnetic moment (a), the period of intervals under consideration increases, the number of intervals corresponding to remagnetization and the pulse duration range in which nanoparticle remagnetization is possible become limited. In the case of a weak bias magnetic field opposite to the initial magnetic moment orientation (c), relative narrowing of intervals corresponding to system nonremagnetization is observed, and the pulse duration range in which remagnetization is absent also becomes limited. Similar diagrams were also presented in [17] for describing experimental data on pulsed remagnetization of a magnetically isotropic film microcell.

Additional studies showed that the alternation of remagnetization/nonremagnetization intervals, arising under the condition $h_0 > k_u$ (without bias magnetic field), takes place is the case of a step field pulse as well. To reveal the general feature, we consider more complex pulse profiles, i.e., harmonically modulated short Gaussian pulses,

$$h(\tau) = h_0 \cos(\Omega\tau) \exp[-(\tau - \tau_i)^2/2\tau_0^2], \qquad (9)$$

where Ω is the dimensionless pulse modulation frequency. Figure 2 shows the diagrams of the dependence of the Y-component of the nanoparticle magnetic moment after relaxation on the pulse amplitude at its duration $\tau_0 = 10$ and modulation frequencies Ω = 0, 0.05, 0.07, 0.09, 0.1, 0.11, 0.2, 0.3 (diagrams 1–8); pulse shapes are shown to the left of diagrams. Since the initial state of the magnetic moment is $\mu_y = 1$, $\mu_x = \mu_z = 0$, these diagrams reveal the pulse duration intervals corresponding to the absence of remagnetization ($\mu_y = 1$) and the implementation of 180-degree remagnetization of the magnetic moment ($\mu_y = -1$). In the case of very short "intervals" obtained by numerical

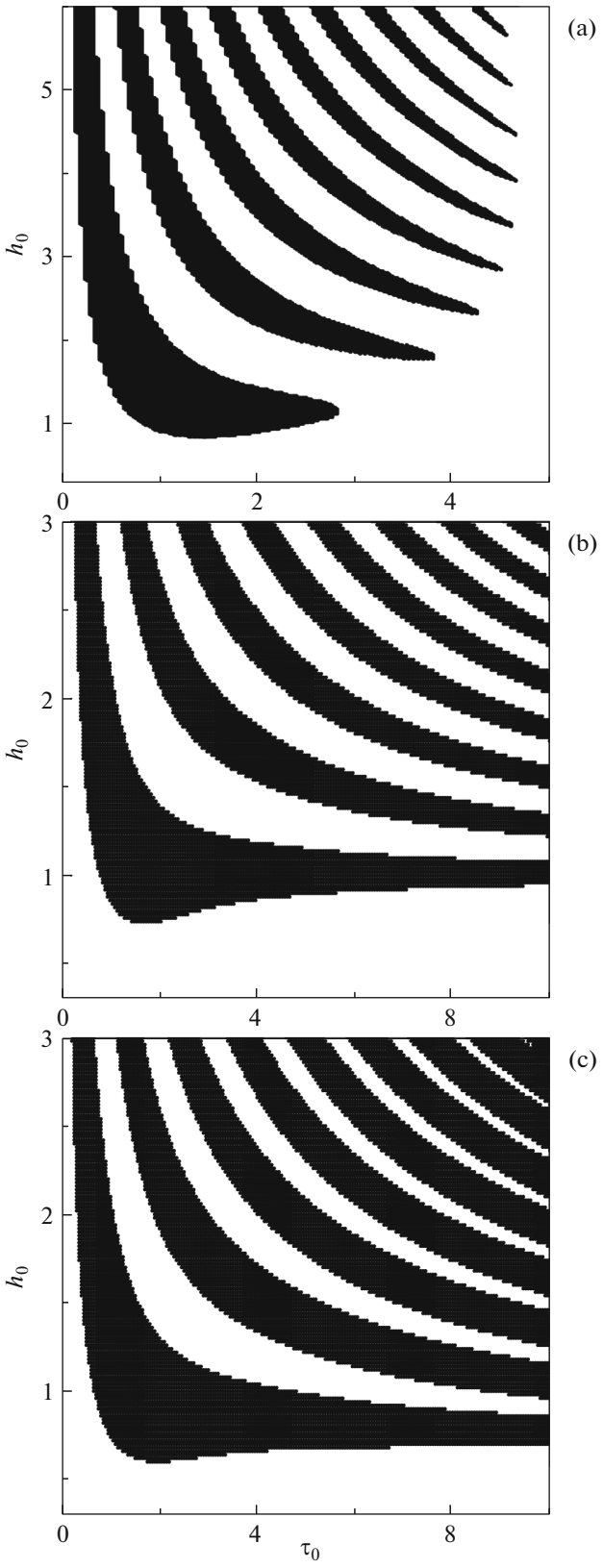

Fig. 1. Diagrams of the dependence of the nanoparticle remagnetization implementation on the pulse amplitude and duration at bias magnetic fields h_y = 0.1, 0, –0.1 (a–c) and the anisotropy constant k_u = 1; dark areas correspond to nanoparticle remagnetization.

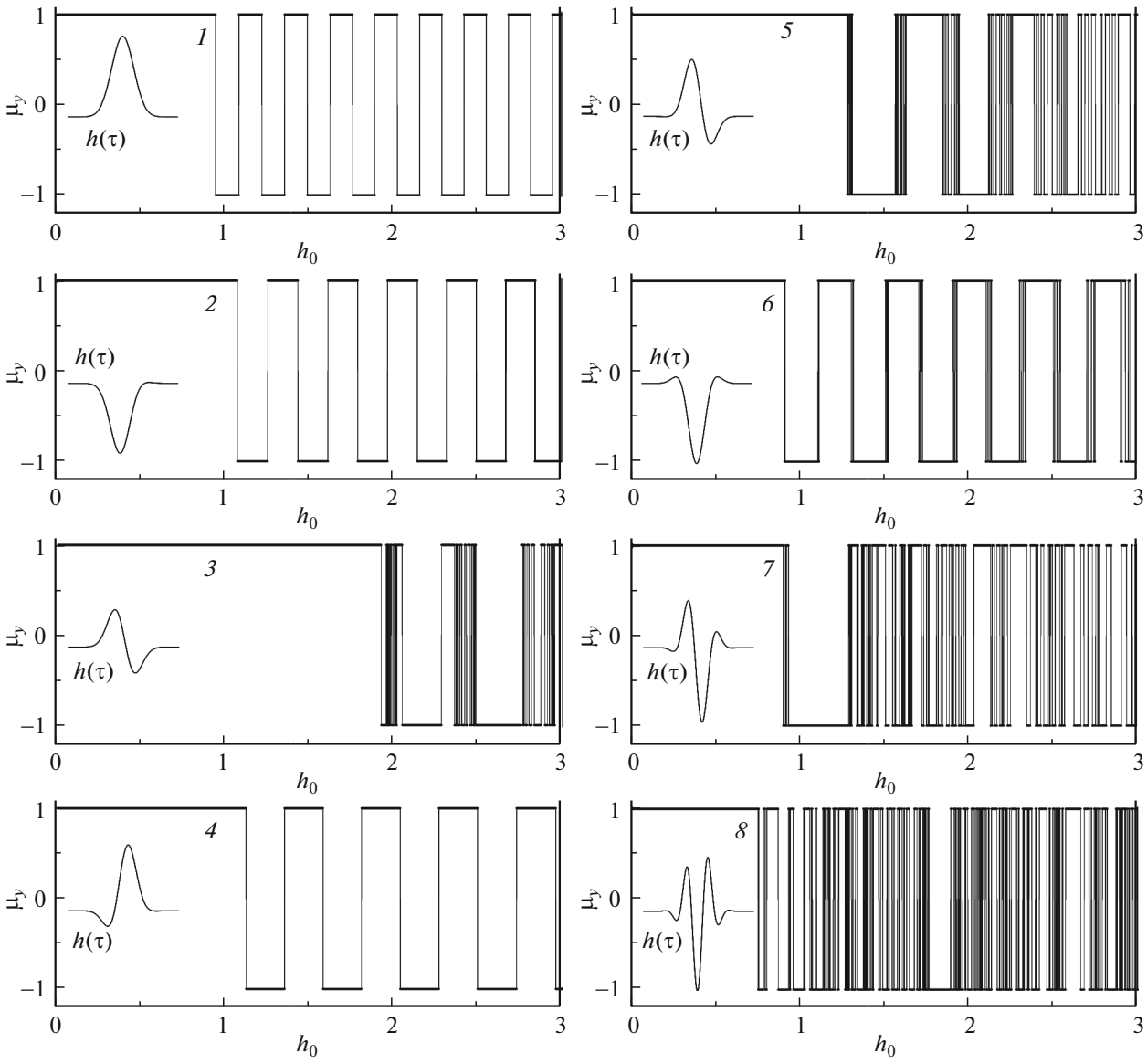

Fig. 2. Diagrams of the dependence of the nanoparticle remagnetization on the Gaussian pulse amplitude at its modulation frequency $Q = 0$, 0.05, 0.07, 0.09, 0.1, 0.11, 0.2, 0.3 (*1*–*8*) and $\tau_0 = 10$; the pulse shapes are shown to the left of diagrams; intervals with $\mu_y = 1$ correspond to the absence of remagnetization, intervals with $\mu_y = -1$ correspond to the magnetization implementation; the close positions of vertical limiting lines correspond to bistability.

simulation, i.e., at close positions of vertical limiting lines in diagrams, bistability takes place. This means that the magnetic moment can either return to the initial position after the pulse action or reverse the direction (the implementation of this or that result depends on fluctuations of system parameters). We can see in diagrams that the response to an unmodulated pulse (1) is characterized by the narrowest remagnetization/nonremagnetization intervals and the complete absence of bistability. In the case of a significant prevalence of one pulse modulation halfwave (2, 4, 6), the close-to-periodic alternation of remagnetization/nonremagnetization intervals is observed as well, and bistability either is absent or takes place in relatively narrow regions near interval boundaries.

In other cases of modulated pulses, bistability intervals become dominant increasing with the pulse amplitude (3, 5) and coalesce into broad bistability bands with increasing modulation frequency.

Figure 3 shows the time dependence of the magnetic moment *Y*-component after exposure to a pulse with the parameters: duration $\tau_0 = 10$, modulation frequency $\Omega = 0.1$, and amplitude $h_0 = 2$ (curve *1*), (curves *2* and *3*). The parameters chosen for the first case correspond to the absence of bistability. In this

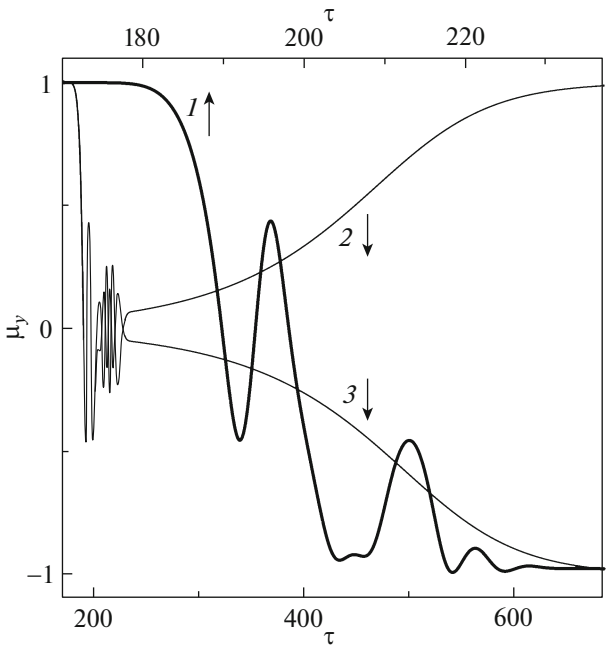

Fig. 3. Time dependence of the magnetic moment *Y*-component upon exposure to the pulse with $\tau_0 = 10$, $h_0 = 2$ (*1*), $h_0 = 2.2$ (*2* and *3*) and the modulation frequency $Q = 0.1$; curves *2* and *3* correspond to the bistability implemented by a small shift of the pulse envelope maximum: $\tau_i = 200$ (for curve *2*) and $\tau_i = 201$ (for curve *1*); the dissipation parameter is $\alpha = -0.01$.

case, fast nanoparticle remagnetization (for the time $\Delta\tau < 60$) is implemented. In the second and third cases, bistability takes place, i.e., the nanoparticle can remagnetize and retain its initial orientation. In this case, the response is prolonged ($\Delta\tau \geq 500$). In the numerical simulation, the bistability manifestation was implemented by a small temporal shift (by unity) of the pulse envelope maximum, which is equivalent to fluctuations of initial conditions.

The remagnetization processes strongly depend on the pulse field direction. Figure 4 shows the diagrams of the dependence of the equilibrium value of the nanoparticle magnetic moment *Y*-component on the amplitude of the Gaussian unmodulated pulse with $\tau_0 = 10$, when the pulse field direction is at a close-to-normal angle to the EMA (*Y* axis): $\varphi = 89°$, 88°, 92°, 100° (diagrams *1–4*, respectively). We can see that even at a one-degree deviation from the normal to the initial magnetic moment orientation, intervals corresponding to nanoparticle remagnetization become substantially narrower; at a two-degree deviation, remagnetization occurs in four very narrow intervals of the pulse amplitude. In the case of an opposite field deviation, similar changes occur at slightly larger angles: at a two-degree deviation, intervals corresponding to nanoparticle nonremagnetization become appreciably narrower; at a 10° deviation, magnetic

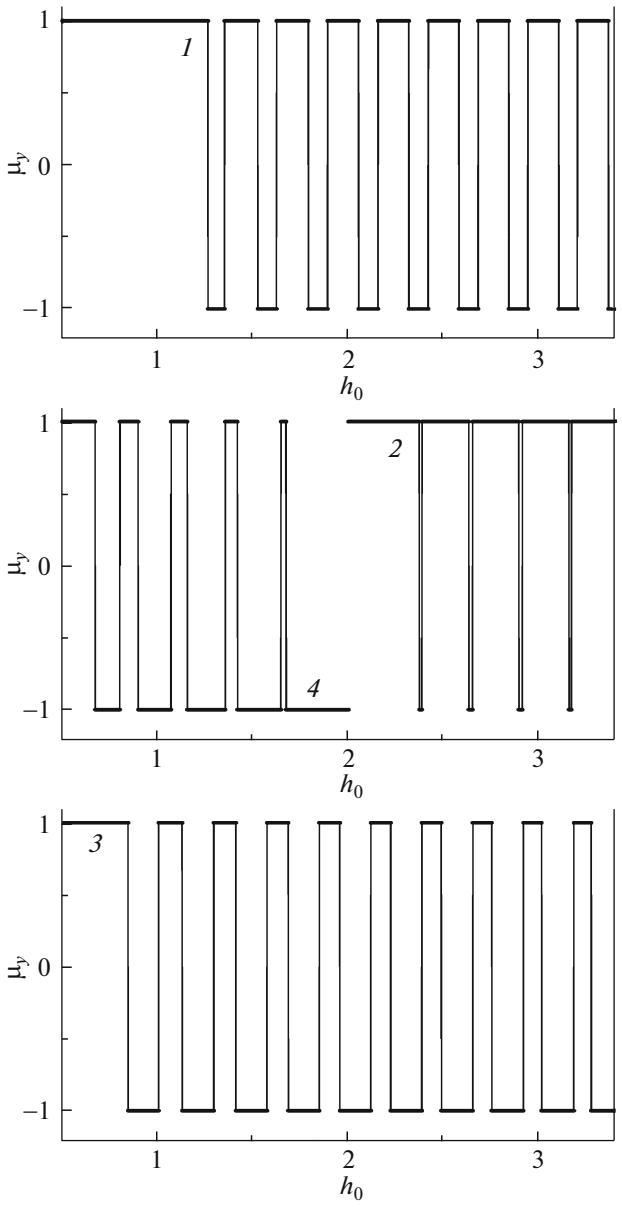

Fig. 4. Diagrams of the dependence of the nanoparticle remagnetization on the amplitude of the Gaussian pulse with $\tau_0 = 10$ at the pulse field direction to the anisotropy axis at angled $\varphi = 89°$, 88°, 92°, 100° (diagrams *1–4*).

moment returns to the initial direction only in four intervals (except for that adjacent to the zero value).

4. RESPONSE DURATION

The precession dynamics of the magnetic moment after the field pulse also intricately depends on the pulse parameters. Figure 5 shows the time dependence of *X*-components of the nanoparticle magnetic moment upon exposure to the Gaussian pulse with $\tau_0 = 1$ and amplitude $h_0 = 0.9$, 1.1, 1.5, 1.9, 2.1 (curves *1–5*).

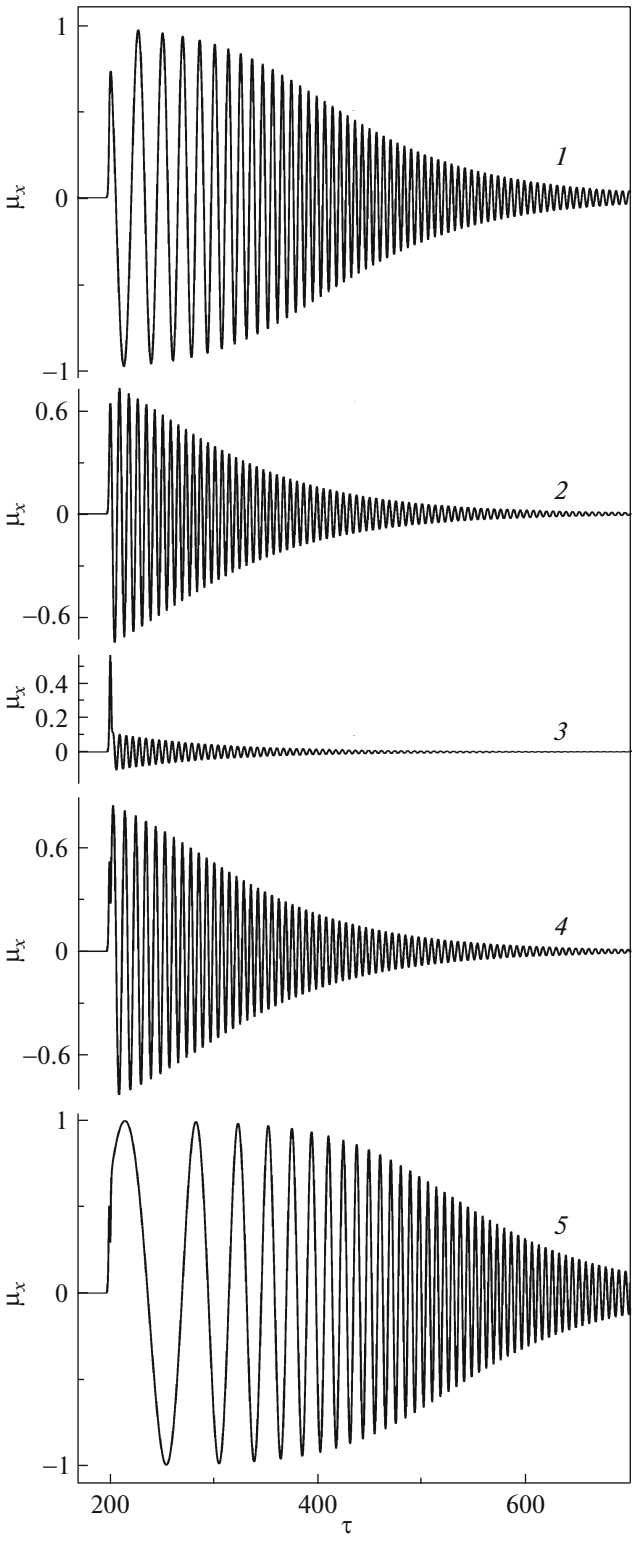

Fig. 5. Time dependence of magnetic moment *X*-components of the nanoparticle with $k_u = 1$ upon exposure to the pulse with $\tau_0 = 1$ and the values $h_0 = 0.9, 1.1, 1.5, 1.9, 2.1$ (curves *1*–*5*) corresponding to movement from one remagnetization interval boundary to the other.

The chosen pulse parameters correspond to the movement from the left boundary of the interval h_0 corresponding to nanoparticle remagnetization to its right boundary (when passing from curve *1* to *5*). We can see in Fig. 5 that the precession response of the magnetic moment to the pulsed action near the interval boundaries (curves *1* and *5*) has a larger amplitude and is hundred times longer than the response at pulse parameters corresponding to the central region of this interval (curve *3*). Similar dependences of the response of the magnetic moment of an isolated nanoparticle on the pulse duration were studied for both anisotropic and isotropic cases in [28].

Figure 6 shows the diagrams defining the dependence of the magnetic moment *Y*-component on the pulse amplitude for the time $\tau = 250$ at pulse duration $\tau_0 = 1, 2, 5$ (diagrams *1*–*3*). The diagrams revealing the nanoparticle remagnetization/nonremagnetization intervals are also shown (lower/upper horizontal segments). The diagrams show that the magnetic moment rapidly comes to the final direction (*Y* or *–Y*, depending on the h_0 interval) in central regions of pulse parameter interval, corresponding to nanoparticle remagnetization and nonremagnetization, since the *Y*-component is approximately equal to ± 1 even at the chosen time ($\tau = 250$). As a result, the magnetic moment response to the pulsed action appears short. However, near the boundaries of these at $\tau = 250$, $|\mu_y| \ll 1$, hence, the magnetic moment precession in the *XZ* plane performed after the pulse has a higher amplitude at a given time, and the response to the pulse momentum is prolonged. We can also see that the shape of the diagrams under study comes close to stepwise with increasing pulse duration along with shortening intervals controlling remagnetization. This means that boundary regions corresponding to the prolonged response of the magnetic moment relatively decrease, and the response to the pulsed action appears short in most intervals.

To explain the revealed effects, Fig. 7 shows projections of magnetic moment trajectories onto the *YZ* plane upon exposure to a pulse of duration $\tau_0 = 5$ and amplitude $h_0 = 2.74$, 2.6, 2.85, and 3 (curves *a*–*d*). The values $h_0 = 2.6$ and 2.85 are in central regions of intervals corresponding to nanoparticle remagnetization and nonremagnetization, and the values $h_0 = 2.74$ and 3 are near the interval boundary. If the pulse action ceases when the magnetic moment *Y*-component is small (*a* and *d*), the magnetic moment begins to precess under the anisotropy field approaching the *Y* axis. As a result, a prolonged magnetic moment response is implemented. But if the pulse action ceases when the *Y*-component is close to ± 1 (*b* and *c*), precession motion under the anisotropy field almost do not arise, and the response appears short. Denoting the positive and negative directions of the *Y* axis by "initial" and "opposite" "poles" of the configuration, and denoting the *XZ* pole to be "equatorial," we can

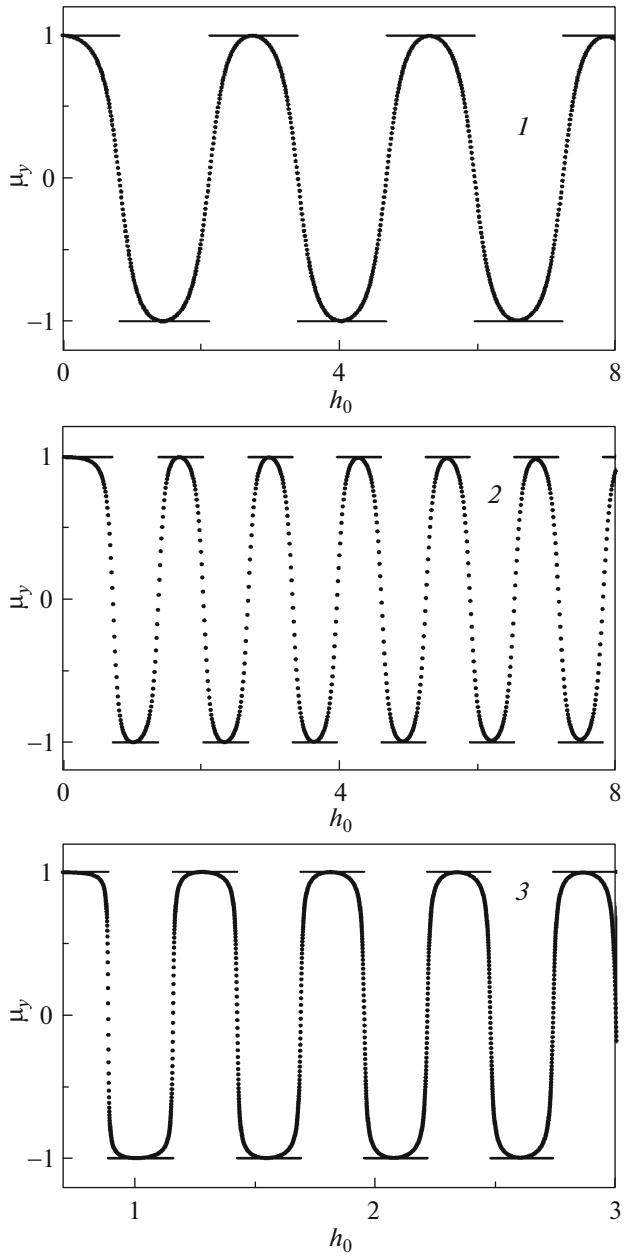

Fig. 6. Diagrams of the dependence of the magnetic moment *Y*-component on the amplitude of the pulse with $\tau_i = 200$ and $h_0 = 1, 2, 5$ (diagrams *1–3*) at the time point $\tau = 250$; lower/upper horizontal segments correspond to nanoparticle remagnetization/nonremagnetization intervals.

say the following. A prolonged response without remagnetization takes place when the magnetic moment after ceasing the pulse action is oriented near the equatorial plane on the initial pole side (*a*).

If the magnetic moment appears near the equatorial plane on the opposite pole side, a prolonged response with remagnetization is implemented (*d*).

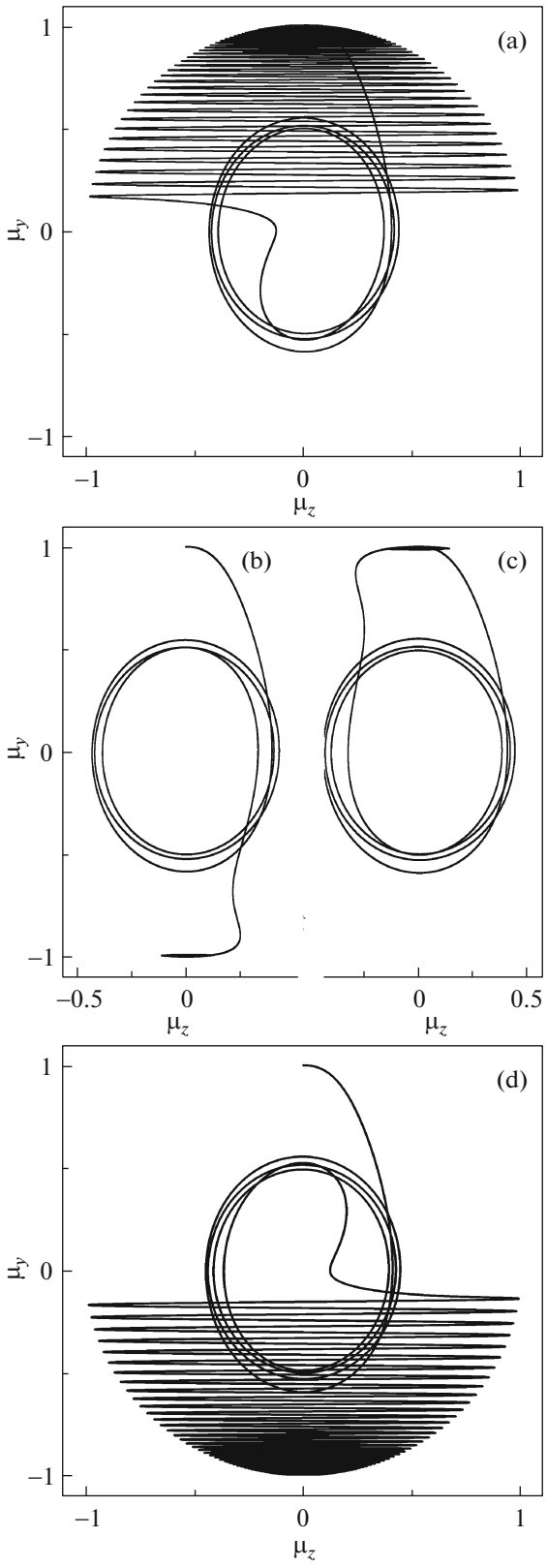

Fig. 7. Projections of nanoparticle magnetic moment trajectories onto the *YZ* plane upon exposure to the pulse with $\tau_0 = 5$ and $h_0 = 2.74, 2.6, 2.85, 3$ (curves a–d).

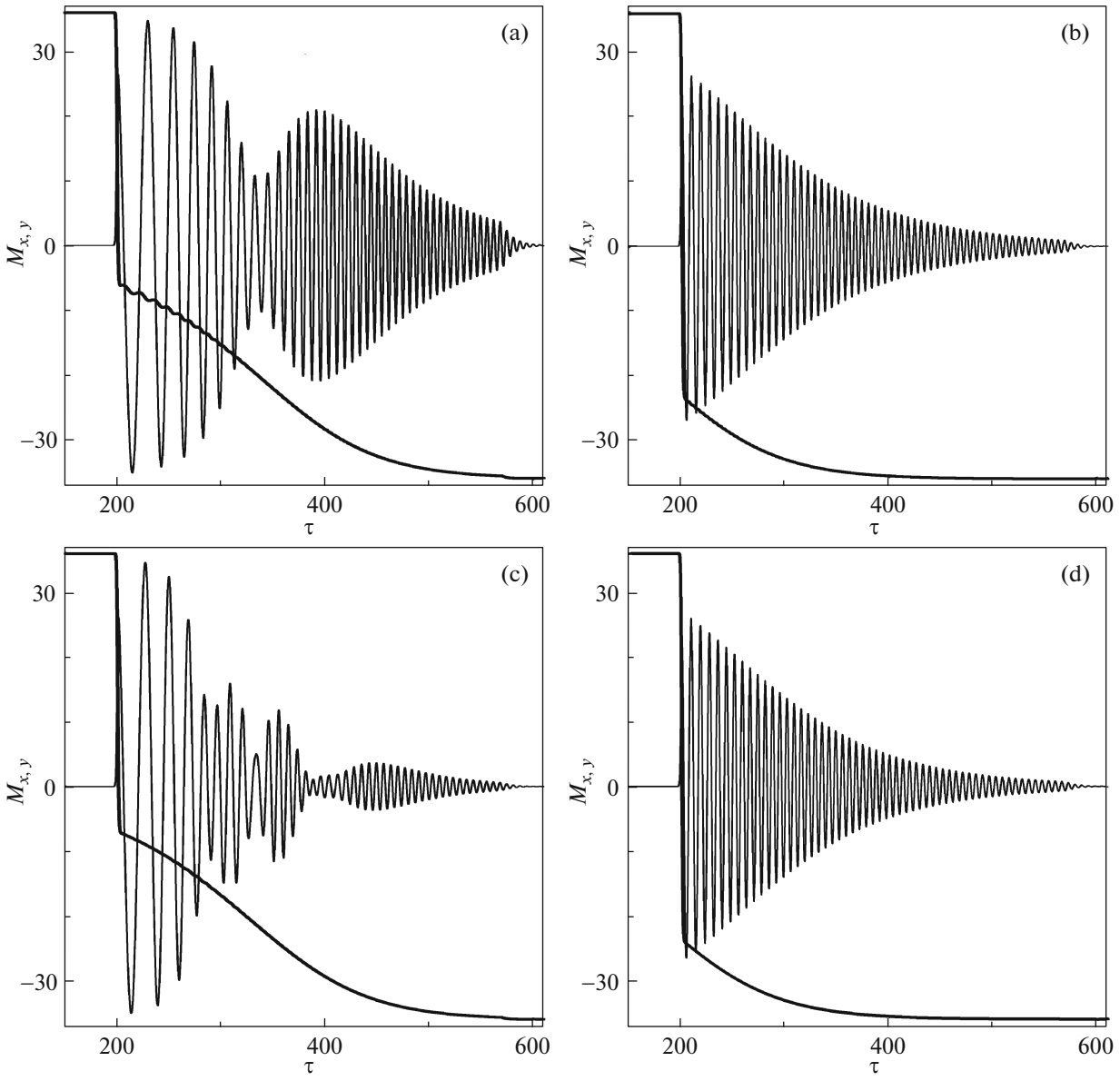

Fig. 8. Time dependence of the magnetic moment components of the 6 × 6 array with parameter $p = 10$ during remagnetization by a pulse with $\tau_0 = 1$, $\tau_i = 200$, $h_0 = 0.9$ (a, c), and $h_0 = 1.1$ (b, d); in the cases (a, b), the EMA coincides with the Y axis, the pulse field is directed along the X axis; in the cases (c, d), the EMA coincides with the X axis, and the pulse field coincides with the Y axis.

But if the working pulse brings the magnetic moment to the region near one of poles, the response is short.

5. MAGNETIC DIPOLE ARRAY RESPONSE TO THE FIELD PULSE

All revealed features of pulsed remagnetization of magnetically uniaxial nanoparticles are also valid for the array at a sufficiently weak dipole–dipole interaction (when the dimensionless array parameter $\rho \geq 5$). For the nanoparticle array 6 × 6 with parameter $\rho = 10$, Fig. 8 shows the time dependence of X, Y-components of the total magnetic moment $\mathbf{M} = \Sigma\boldsymbol{\mu}_i$ upon exposure to the Gaussian pulse with $\tau_0 = 1$ and $h_0 = 0.9$ (a, c), which corresponds to the boundary region of the remagnetization interval, and $h_0 = 1.1$ (b, d), which corresponds to the region slightly closer to the interval center. To compare various configurations in the cases (a, b), the previous geometry was taken (the anisotropy axis coincides with the Y axis and the pulse field is directed along the X axis). But in the cases (c, d), it is accepted that the uniaxial anisotropy direction coincides with the X axis perpendicular to the array plane; in the initial state, all array magnetic moments are

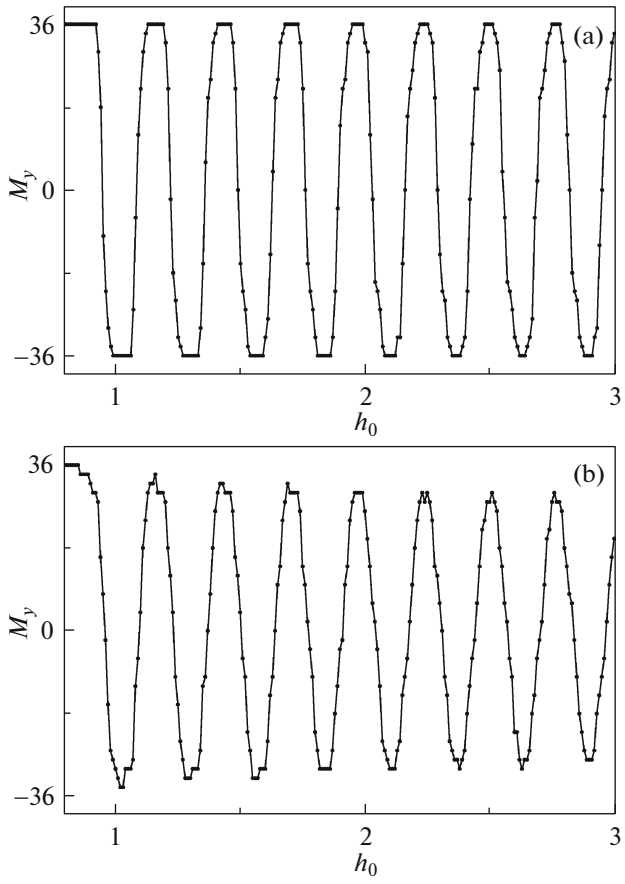

Fig. 9. Diagrams of the dependence of the equilibrium value of the magnetic moment *Y*-components of the array 6×6 with $p = 10$ on the pulse amplitude in the case of nanoparticle spread over EMA angles 0 and φ of with root-mean-square deviations of (a) 1° and (b) 2°.

directed in the positive direction of the *X* axis, and the pulse field is oriented along the *Y* axis. A comparison of this figure with Fig. 5 for the isolated nanoparticle, we can see that the weak dipole–dipole interaction manifests itself by the appearance of precession motion modulation. Therewith the influence of neighboring dipoles is appreciable only near the remagnetization interval boundary (*a*, *c*), and is stronger in the case of perpendicular configuration (*c*). At the pulse parameters corresponding to the central region of remagnetization/nonremagnetization intervals, hence, at a short response to the pulse, the dipole–dipole interaction effect appears only at small array parameters, when the homogeneous equilibrium configuration loses stability.

In the case of the presence of EMA spread of a nanoparticle entering the array, with respect to the average direction controlled by external conditions, system remagnetization diagrams vary depending the angular dispersion. In this case, an analysis shows that the spread over the azimuthal angle φ measured from the *Y* axis in the *YZ* array plane (at the considered perpendicular orientation of the pulse field and weak dipole–dipole interaction) almost has no effect on the precession dynamics of the system response and remagnetization. But the EMA spread over the polar angle θ measured from the array plane significantly affects the response and final orientation of individual dipoles of the system, as follows from Fig. 4.

Figure 9 shows the diagrams of the dependence of the equilibrium value of the *Y*-component of the total magnetic moment of the nanoparticle array 6×6 with parameter $\rho = 10$ on the amplitude of the working pulse with $\tau_0 = 10$. The diagrams correspond to the normal (Gaussian) distribution of anisotropy angles over angles θ and φ with root-mean-square deviations of 1° and 2° (*a*, *b*). We can see that regions of partial array remagnetization appear between regions of complete remagnetization/nonremagnetization in the case (*a*); therewith, the width of the latter narrows with increasing pulse amplitude, and complete remagnetization (and nonremagnetization) will be absent at sufficiently large h_0. As the variance over anisotropy angles increases (*b*), complete remagnetization and nonremagnetization of the array is not implemented, and close-to-periodic variations (with increasing one of the pulse parameters) in the number of nanoparticles remagnetized under the pulse action take place.

6. CONCLUSIONS

The study of the response of the magnetic moment of the nanoparticle with uniaxial anisotropy to the short Gaussian magnetic field pulse revealed the strong dependence of remagnetization implementation and precession dynamics duration on the pulse duration and peak value. As the pulse amplitude or duration varies, the magnetic moment response duration periodically reaches its maximum and minimum values. Under the conditions corresponding to the minimum of the magnetic moment response to the pulse action, after a short precession dynamics burst, the phase trajectory rapidly approaches the equilibrium state. The response maxima divide the pulse parameter domain into intervals corresponding to nanoparticle remagnetization, which alternate with intervals corresponding to the absence of remagnetization. In this case, central regions of intervals are characterized by short magnetic moment responses, while edge regions exhibit prolonged responses. The width of these parametric remagnetization/nonremagnetization intervals is reduced with increasing the pulse duration or the pulse peak over the uniaxial anisotropy constant.

The revealed features of the nanoparticle and array response to the pulsed action are caused by the nature of attractors of precession motion or the magnetic moment of the nonlinear system under consideration. The response duration and the remagnetization implementation are controlled by the magnetic

moment position with respect to the anisotropy axis after the pulse end. In the case of a modulated pulse, the alternation of parametric remagnetization/nonremagnetization intervals arises only in the case of a significant prevalence of one modulation halfwave in the pulse. In other cases, extensive bistability regions take place, when the magnetic moment can either return to the initial state and come to the opposite orientation after the pulse due to various fluctuations.

The bias magnetic field directed along the nanoparticle EMA has a strong effect on remagnetization processes. Using a weak field, pulse parameter domains corresponding to either remagnetization or nonremagnetization of nanoparticles can be significantly restricted. A similar effect is caused by a pulse field deviation by several degrees from the normal to the EMA; the strongest effect on remagnetization processes has the deviation to the direction coinciding with the initial orientation of magnetic moments.

In the case of nanoparticle arrays, the weak dipole–dipole interaction leads to modulation of the precession dynamics of the total magnetic moment. This appears to a greater extent in the case of the perpendicular configuration where the easy axis coincides with the normal to the array plane. However, the effect of the dipole–dipole interaction on the precession dynamics appears only near boundaries of the above intervals of pulse parameters in both configurations. In the case of the angular EMA spread of individual array nanoparticles distributed by the Gaussian law with the root-mean-square deviation $\Delta\theta_i \geq 1°$, only partial array remagnetization is implemented. Therewith, with varying pulse parameters, a close to periodic variation in the number of remagnetized nanoparticles takes place.

The results obtained reveal the general nature of pulsed remagnetization of dipole systems with uniaxial anisotropy, which confirms previous experimental studies of other magnetic structures.

FUNDING

This study was supported by the Ministry of Science and Education of the Russian Federation (State contract no. 3.6825.2017/BCh) and the Russian Foundation for Basic Research (project no. 18-42-730001/18).

CONFLICT OF INTEREST

The authors declare that they have no conflicts of interest.

REFERENCES

1. R. Skomski, J. Phys.: Condens. Matter. **15**, R841 (2003).
2. E. Z. Meilikhov and R. M. Farzetdinova, J. Magn. Magn. Mater. **268**, 237 (2004).
3. Yu. P. Ivanov, A. I. Il'in, E. V. Pustovalov, and L. A. Chebotkevich, Phys. Solid State **52**, 1694 (2010).
4. V. A. Kosobukin and B. B. Krichevtsov, Phys. Solid State **52**, 813 (2010).
5. P. V. Bondarenko, A. Yu. Galkin, and B. A. Ivanov, J. Exp. Theor. Phys. **112**, 986 (2011).
6. A. A. Fraerman, Phys. Usp. **55**, 1255 (2012).
7. S. A. Dzian and B. A. Ivanov, J. Exp. Theor. Phys. **115**, 854 (2012).
8. S. A. Gudoshnikov, B. Ya. Liubimov, A. V. Popova, and N. A. Usov, J. Magn. Magn. Mater. **324**, 3690 (2012).
9. T. Kiseleva, S. Zholudev, A. Novakova, and T. Grigoryeva, Comp. Struct. **138**, 12 (2016).
10. M. F. Hansen, P. E. Jonsson, P. Nordblad, and P. Svedlindh, J. Phys.: Condens. Matter **14**, 4901 (2012).
11. A. M. Shutyi and D. I. Sementsov, Phys. Solid State **60**, 2471 (2018).
12. A. M. Shutyi and D. I. Sementsov, JETP Lett. **99**, 695 (2014).
13. A. M. Shutyi, S. V. Eliseevay, and D. I. Sementsov, Phys. Rev. B **91**, 024421 (2015).
14. A. M. Shutyi and D. I. Sementsov, J. Magn. Magn. Mater. **401**, 1033 (2016).
15. N. Eibagi, J. J. Kan, F. E. Spada, and E. E. Fullerton, IEEE Magn. Lett. **3**, 4500204 (2012).
16. E. Z. Meilikhov and R. M. Farzetdinova, Phys. Solid State **56**, 2408 (2014).
17. H. W. Schumacher, C. Chappert, P. Crozat, R. C. Sousa, P. P. Freitas, J. Miltat, J. Fassbender, and B. Hillebrands, Phys. Rev. Lett. **90**, 017201 (2003).
18. H. W. Schumacher, C. Chappert, R. C. Sousa, P. P. Freitas, J. Miltat, and J. Fassbender, Phys. Rev. Lett. **90**, 017204 (2003).
19. A. V. Kimel, B. A. Ivanov, R. V. Pisarev, P. A. Usachev, A. Kirilyuk, and Th. Rasing, Nat. Phys. **5**, 727 (2009).
20. T. Satoh, Sung-Jin Cho, R. Iida, Ts. Shimura, K. Kuroda, H. Ueda, Yu. Ueda, B. A. Ivanov, F. Nori, and M. Fiebig, Phys. Rev. Lett. **105**, 077402 (2010).
21. A. Yu. Galkin and B. A. Ivanov, JETP Lett. **88**, 249 (2008).
22. Yu. I. Dzhezherya, V. P. Yurchuk, K. O. Demishev, and V. N. Korenivskii, J. Exp. Theor. Phys. **117**, 1059 (2013).
23. A. Sukhov and J. Berakdar, Phys. Rev. B **79**, 134433 (2009).
24. V. V. Randoshkin, A. M. Saletsky, N. N. Usmanov, and D. B. Chopornyak, Phys. Solid State **46**, 474 (2004).
25. E. I. Il'yashenko, O. S. Kolotov, A. V. Matyunin, O. A. Mironets, and V. A. Pogozhev, Tech. Phys. **51**, 1534 (2006).
26. D. A. Balaev, A. A. Krasikov, D. A. Velikanov, S. I. Popkov, N. V. Dubynin, S. V. Stolyar, V. P. Ladygina, and R. N. Yaroslavtsev, Phys. Solid State **60**, 1973 (2018).
27. A. G. Gurevich and G. A. Melkov, *Magnetic Oscillations and Waves* (Nauka, Moscow, 1994) [in Russian].
28. A. M. Shutyi and D. I. Sementsov, JETP Lett. **108**, 740 (2018).

Translated by A. Kazantsev